

Influence of Crystal Structure on the Fatigue Properties of $\text{Pb}_{1-x}\text{La}_x(\text{Zr}_y\text{Ti}_z)\text{O}_3$ Thin Films Prepared by Pulsed-Laser Deposition Technique

Wen-Jen Lin and Tseung-Yuen Tseng*

Department of Electronics Engineering and Institute of Electronics, National Chiao-Tung University, 300 Taiwan, Republic of China

Sheuan-Perng Lin, Shun-Lih Tu, Hong Chang, and Sheng-Jenn Yang

Materials Research and Development Center, Chung Shan Institute of Science and Technology, Taiwan, Republic of China

I-Nan Lin

Materials Science Center, National Tsing-Hua University, 300 Taiwan, Republic of China

Lead lanthanum zirconate titanate ($\text{Pb}_{1-x}\text{La}_x(\text{Zr}_y\text{Ti}_z)\text{O}_3$, PLZT) films containing [00 l] preferentially oriented grains were produced successfully on $\text{YBa}_2\text{Cu}_3\text{O}_{7-x}$ -coated (YBCO-coated) SrTiO_3 (STO) or YBCO/ CeO_2 -coated silicon substrates; films containing randomly oriented grains were created on platinum-coated silicon substrates. The latter possessed significantly inferior ferroelectric properties, a fact ascribed to the presence of a paraelectric phase (TiO_2) at the PLZT/platinum interface. On the other hand, the PLZT/YBCO/STO films exhibited better electrical properties than did the PLZT/YBCO/ CeO_2 /Si films, and this phenomenon was attributed to better alignment of the grains in normal and in-plane orientations. In terms of fatigue properties, the [00 l] textured films that were deposited on YBCO/ CeO_2 /Si substrates possessed substantially superior polarization-switching-cycle endurance versus the randomly oriented films grown on Pt(Ti)/Si substrates. Moreover, the tetragonal films behaved much more satisfactorily than did the rhombohedral PLZT films. The ferroelectric parameters of tetragonal PLZT films showed no significant degradation up to 10^9 polarization switching cycles, whereas the remnant polarization and coercive force of the rhombohedral PLZT films had already degraded to 80% of their initial values after 10^8 cycles.

I. Introduction

RECENTLY, growing interest has focused on dielectric and ferroelectric thin films for applications in dynamic random access memory (DRAM)^{1,2} and nonvolatile ferroelectric random access memory (FRAM) technologies.³⁻⁶ Reliability problems such as polarization fatigue, which refers to a decrease in the remnant polarization (P_r) with increasing switching cycles, are the main obstacle to applying these devices as well as to integrating them with a semiconductor process. Thus, extensive research has been addressed to this issue.²⁻¹²

Previous studies focused on the degradation of polarization, as related to defects within the materials.⁵⁻⁸ No mention was

made of the correlation between the crystal structure of the films and their fatigue properties. However, cyclic polarization switching, which induces repeated strain because of the piezoelectricity of the materials, has been observed to cause reliability problems in multilayer lead zirconate titanate (PZT).¹³ The same phenomenon also may occur in ferroelectric thin films.

The goal of the present paper is to investigate the possible influence of piezoelectrically induced strain on the polarization fatigue of ferroelectric films. For this purpose, lead lanthanum zirconate titanate ($\text{Pb}_{1-x}\text{La}_x(\text{Zr}_y\text{Ti}_z)\text{O}_3$, PLZT) films of either tetragonal (T) or rhombohedral (R) structure, preferentially oriented in the [00 l] direction, have been grown on a silicate substrate. Degradation of the ferroelectric properties of these films with increasing switching cycles is examined, and the correlation of these characteristics will be discussed.

II. Experimental Procedure

The laser beam from a KrF laser (248 nm, Model LPX200, Lambda Physik, Goettingen, FRG) with an energy density of 3.5 J/cm² was used for growing PLZT films via a pulsed-laser deposition technique. Targets of composition $\text{Pb}_{1-x}\text{La}_x(\text{Zr}_y\text{Ti}_z)\text{O}_3$ with $x = 0.03$ and an $x:y:z$ ratio of either 3:54:46 or 3:34:66 were prepared via a chemical route. Those PLZT materials were rhombohedral (R) or tetragonal (T) in structure, respectively, in bulk ceramic form. The PLZT films were deposited at 500°–600°C, with an oxygen pressure (p_{O_2}) that was controlled in the range of 1–100 Pa. The substrates that were used for growing the PLZT were platinum-coated silicon (Pt(Ti)/Si), $\text{YBa}_2\text{Cu}_3\text{O}_{7-x}$ -coated SrTiO_3 (YBCO/STO) or YBCO-coated silicon with CeO_2 as a buffer layer (YBCO/ CeO_2 /Si). The YBCO layer was applied at 750°C under 50 Pa of oxygen pressure, and CeO_2 layer was deposited at 700°C under 10 Pa of oxygen pressure.

The crystal structure of the PLZT films and the alignment of the a - and b -axes on the film surfaces were examined by X-ray diffractometry (XRD) (Model DMAX-IIIB, Rigaku Co., Tokyo, Japan, with a $\text{CuK}\alpha$ source) and by a ϕ -scan XRD technique, respectively. The morphology of the thin-film surface was investigated by atomic force microscopy (AFM) (Model Nanoscope-III, Digital Instruments, Santa Barbara, CA). The interfaces of the films were examined by the elemental depth profiling of secondary-ion mass spectroscopy (SIMS) (Model ims-4f, Cameca, Courbevoie Cedex, France). The fatigue of the ferroelectric properties was measured under alternating signals of 5 V (60 Hz), using a modified Sawyer–Tower method. A gold

M. P. Harmer—contributing editor

Manuscript No. 192368. Received August 24, 1995; approved October 23, 1996. Supported by the National Science Council of the Republic of China, under Contract No. NSC 84-2112-M009-028 PH.
*Member, American Ceramic Society.

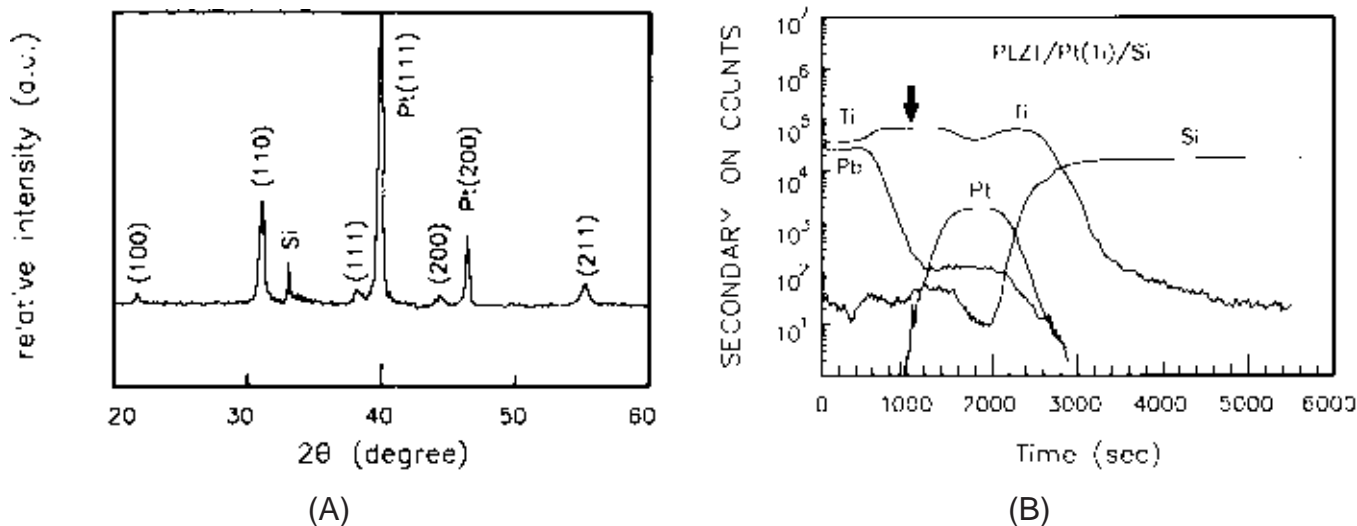


Fig. 1. (A) XRD pattern and (B) SIMS spectrum of PLZT films that have been deposited on Pt(Ti)/Si substrates.

layer patterned by a conventional lithographic technique was used as the top electrode.

III. Results and Discussion

The formation of PLZT thin films on Pt(Ti)/Si substrates is a difficult process, and the ranges of substrate temperature and oxygen pressure p_{O_2} in which a pure perovskite phase can be obtained are quite narrow.¹⁴ Typical XRD patterns of PLZT films that have been grown in the present work on a Pt(Ti)/Si substrate (as shown in Fig. 1(A)) indicate that the films that were deposited onto these substrates were tetragonal, with a small c/a ratio, and polycrystalline, consisting of randomly oriented grains. Moreover, the titanium underlayer, which was precoated onto the silicon to increase the adhesion of the platinum layer, diffused outward during deposition of the PLZT films. This phenomenon was indicated by SIMS (see Fig. 1(B)), where an extraordinarily high titanium ion count could be observed at the interface between the PLZT film and the platinum layer (arrow in Fig. 1(B)). However, interdiffusion between the PLZT films and the silicon was suppressed effectively by the platinum and titanium layers. Although the formation of a TiO_2 layer that was caused by the outward diffusion of the titanium species enhanced the nucleation of the PLZT films,¹⁵ the apparent ferroelectric properties of the films were degraded substantially because of that layer, a fact that will be further discussed shortly.

On the contrary, PLZT films preferentially oriented in the [001] direction were obtained easily on YBCO/STO and YBCO/CeO₂/Si substrates. These films were abbreviated, respectively, as PLZT/STO and PLZT/Si. However, Table I shows that the synthesis of a pure perovskite phase still requires stringent control of the deposition parameters. The pyrochlore phase

formed preferentially in an environment of low substrate temperature (500°C) and high p_{O_2} (100 Pa). The lead-deficient secondary phase, $Zr_{1-x}Ti_xO_2$, was easily induced under a high substrate temperature (~600°C) in conjunction with a low p_{O_2} (~1 Pa).

The XRD patterns of the films that were deposited under optimum conditions, 500°C at 10 Pa or 550°C at 10 Pa, are shown in Figs. 2(A) and (B), where R and T represent films that have been obtained from targets of rhombohedral and tetragonal structure, respectively. An AFM examination indicated that the grain size of all the films was quite small (~0.1 μm) and that the roughness was ~20 nm when the films were deposited onto YBCO/STO substrates. The grain size and roughness were slightly larger (0.2–0.4 μm, 25 nm) for films that were grown on YBCO/CeO₂/Si substrates. Splitting of (001)/(100) or (002)/(200) diffraction peaks in the tetragonal perovskite structure was barely resolved. The suppression of tetragonality in these films was caused partially by the strain induced by substrate–film constraint and partially by the fine-grain nature of the films.

The alignment of the a - and b -axes on the film plane of the PLZT/STO was examined by XRD ϕ -scan for the PLZT(101), YBCO(102), and STO(101) diffraction peaks, as shown in Fig. 2(C). Those results indicate that the a - and b -axes of the PLZT lattices were aligned with those of the YBCO and STO lattices. The full width at half maximum (FWHM, $\Delta\theta$) value for the rocking curve of the (001) diffraction peak of the rhombohedral films ($\Delta\theta_R \approx 1.08^\circ$) was substantially larger than that of the tetragonal films ($\Delta\theta_T \approx 0.28^\circ$). Similar analysis, viz. a ϕ -scan of the PLZT(101) diffraction peaks and the rocking curve of the (001) diffraction peaks, on the PLZT/Si films indicated that the crystallinity of these films was slightly inferior to that of the PLZT/STO films.

Table I. Phase Constituents of Rhombohedral (R) and Tetragonal (T) PLZT Films Deposited under Various Substrate Temperatures and Oxygen Pressures (p_{O_2})

Film [†]	Substrate temperature (°C)	Phase constituent [‡]		
		$p_{O_2} = 100$ Pa	$p_{O_2} = 10$ Pa	$p_{O_2} = 1$ Pa
R	500	π	P	P(π)
R	550	P + π	P(π)	P + π + Z
R	600	P + π	P + π + Z	P + π + Z
T	500	π	P(π)	P + π
T	550	P(π)	P + π	P + π
T	600	P + π	P + π	P + π + Z

[†]R is PLZT with the $x:y:z$ ratio of 3:54:46; T is PLZT with the $x:y:z$ ratio of 3:34:66. [‡] π represents the pyrochlore phase, P represents the perovskite phase, Z represents the $Zr_{1-x}Ti_xO_2$ phase, and P(π) represents the perovskite phase that contains a minimal proportion of pyrochlore phase.

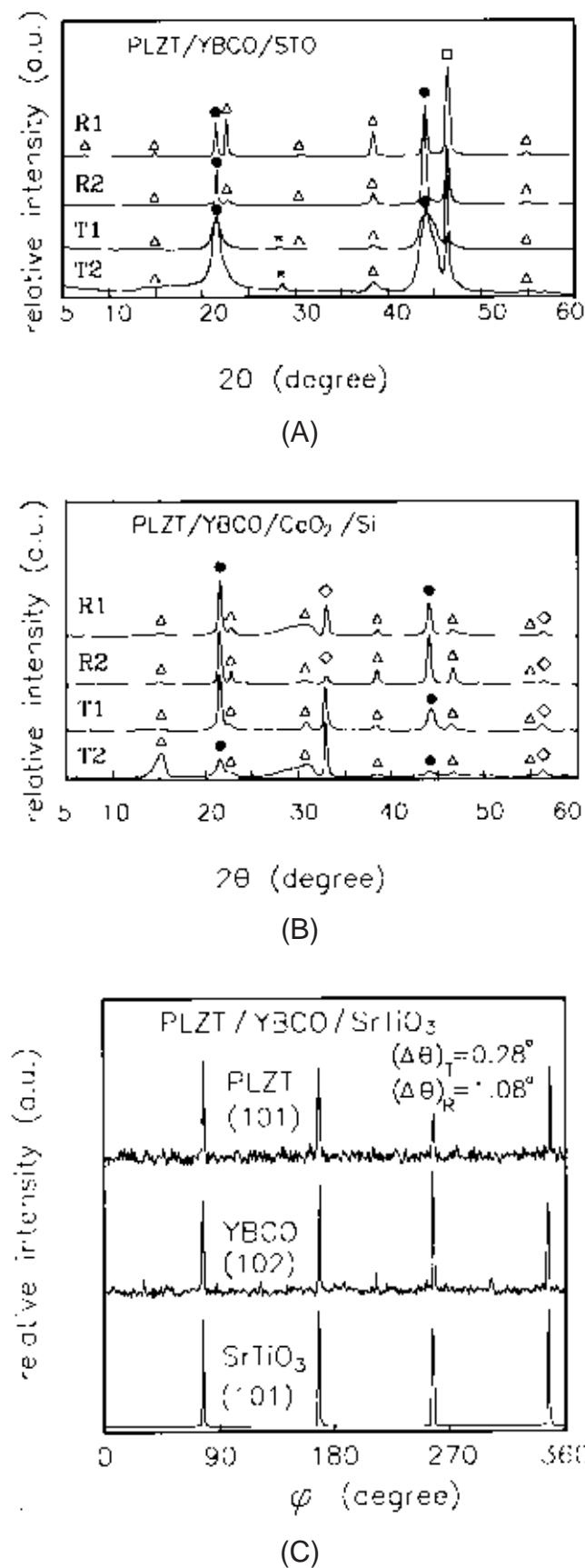


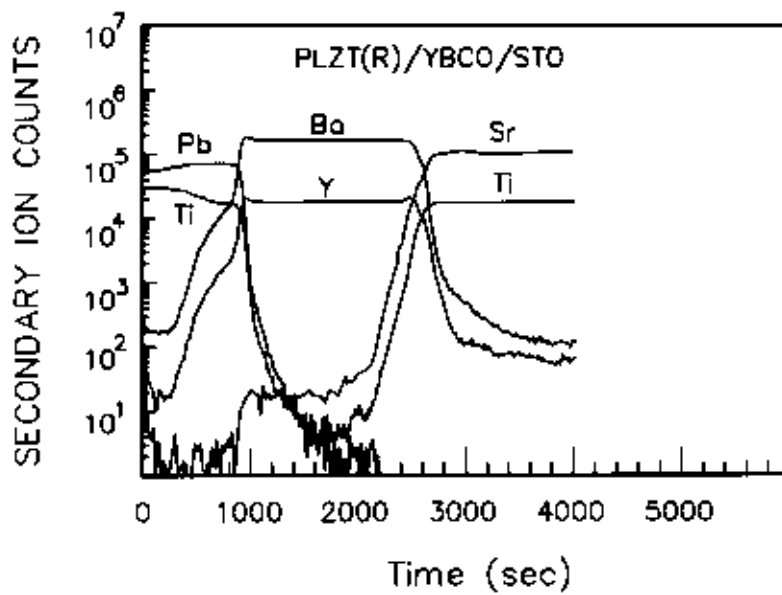
Fig. 2. XRD patterns of rhombohedral (R) and tetragonal (T) films that have been deposited on (A) YBCO/STO or (B) YBCO/CeO₂/Si substrates at 500° (R1 and T1) and 550°C (R2 and T2) under an oxygen pressure of 10 Pa (● PLZT, △ YBCO, □ STO, and ◇ CeO₂); (C) φ-scan of XRD of PLZT(101), YBCO(102), and STO(101) diffraction peaks of PLZT/YBCO/STO films (the corresponding FWHM of the PLZT(001) rocking curve is indicated).

Elemental depth profiles of the PLZT/YBCO/STO and PLZT/YBCO/CeO₂/Si thin films also were examined by SIMS. The spectra are shown in Figs. 3 and 4 for tetragonal and rhombohedral films, respectively. The interface between the PLZT films and the YBCO intermediate layer was very sharp when the films were deposited onto the STO substrates but slightly diffuse when they were grown onto the CeO₂-coated silicon substrates. Such a result indicates that the CeO₂ buffer layer, although completely blocking interdiffusion between the YBCO intermediate layer and the silicon, reacted substantially with the YBCO layer by itself. Misaligned YBCO grains resulted, consequently inducing imperfections in the preferential orientation of the PLZT films and in the sharpness of the PLZT/YBCO interface.

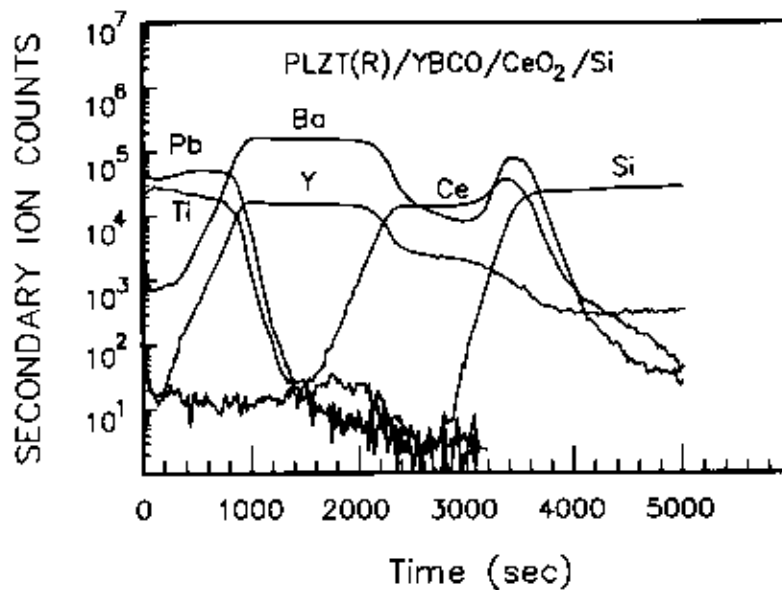
The ferroelectric properties—the P - E curves—of these films, measured by the modified Sawyer-Tower technique, are shown in Fig. 5. The remnant polarization (P_r) and the coercive field (E_c) of the films are listed in Table II. The P_r value for the PLZT films that were deposited onto Pt(Ti)/Si substrates was markedly lower than that of films grown onto YBCO/STO or YBCO/Si substrates, whereas the E_c values were the same for all the films. Smaller P_r values of the PLZT/Pt(Ti)/Si films were caused not only by the random orientation of their grains but also by the presence of a paraelectric TiO₂ layer, which was connected to the ferroelectric PLZT films in series. A comparison of ferroelectric properties among the textured PLZT films revealed that crystal symmetry and the substrate materials both markedly affect P - E behavior. For the films that were deposited onto YBCO/STO, the properties of the tetragonal PLZT, (P_r)_T = 17.8 μC/cm² and (E_c)_T = 56 kV/cm, were better than those of the rhombohedral PLZT, (P_r)_R = 12 μC/cm² and (E_c)_R = 46 kV/cm. On the other hand, the ferroelectric behavior of the rhombohedral PLZT films that were deposited on silicon, (P_r)_R = 11.2 μC/cm² and (E_c)_R = 44.2 kV/cm, was almost as good as that for films grown on STO, whereas the properties of the tetragonal PLZT/Si films, (P_r)_T = 11.8 μC/cm² and (E_c)_T = 40 kV/cm, were markedly lower than those of the tetragonal PLZT/STO films.

The ferroelectric behavior of the [001] textured samples apparently can be correlated with the intrinsic properties that are associated with the ferroelectric crystal symmetry of those materials.¹⁶ The direction of spontaneous polarization for the tetragonal films ($P = [001]$) was aligned with the normal of the film, and that of the rhombohedral films ($P = [111]$) was inclined to it. Thus, the polarization value (P_r) of tetragonal films was markedly larger than that of rhombohedral films. It was difficult to switch the polarization vector from one orientation (e.g., [001]) to the other (e.g., [00 $\bar{1}$]) in tetragonal films. In contrast, the inclined polarization of the rhombohedral films easily switched from one [111] orientation to another. Therefore, a larger coercive force (E_c) could be associated with the tetragonal films and smaller values of this parameter would be associated with the rhombohedral films. The inferior ferroelectric properties of the PLZT/Si films, as compared with those of the PLZT/STO films, indicate the importance of perfect grain alignment. A pronounced PLZT-YBCO interaction also was a possible factor in lowering the electrical properties of the PLZT/Si films.

The degradation of ferroelectric properties, including remnant polarization P_r and coercive force E_c , with the increasing switching cycle—that is, the fatigue properties of the films—was evaluated by applying an ac signal (5 V, 60 Hz) to the samples. Figure 6(A) shows the marked change in the P - E hysteresis curve of the PLZT/Pt(Ti)/Si films (tetragonal) with polarization switching. The P_r value of the samples decreased monotonically as the number of switching cycles increased (Fig. 6(B)). That figure was reduced to ~84% of its initial value (P_r^0) after 10⁸ cycles and further lowered to ~53% of P_r^0 after 10⁹ cycles. The E_c value of the samples, on the other hand, degraded only moderately as polarization switching increased (Fig. 6(C)). In the meantime, the fatigue properties of the [001]



(A)



(B)

Fig. 3. SIMS spectra of tetragonal PLZT films that have been deposited on (A) YBCO/STO and (B) YBCO/CeO₂/Si substrates at 500°C (p_{O_2} = 10 Pa).

textured PLZT films—PLZT/YBCO/STO and PLZT/YBCO/CeO₂/Si—changed pronouncedly as the crystal symmetry of the materials changed.

The structural dependence of the fatigue properties of the PLZT films on YBCO/STO substrates possessed similar behavior as that on YBCO/CeO₂/Si substrates. Therefore, only the latter will be described. Figure 6 reveals that the rhombohedral films degraded markedly because of polarization switching: the P_r value decreased to ~80% of its initial value after 10⁸ switching cycles, whereas the E_C value increased abruptly at 10⁶ switching cycles and decreased inversely after that. In contrast, the P_r and E_C values of the tetragonal films hardly changed, even when the films were cycled with polarization switching up to 10⁹ cycles. However, the fatigue properties of these films were comparable to those reported for PZT films.²⁻¹²

The fatigue of ferroelectric films theoretically is induced by the formation of defects,^{7,8} which can account very well for the rapid degradation of the tetragonal PLZT/Pt(Ti)/Si films. The presence of an outwardly diffused TiO₂ layer also may result in serious PLZT–TiO₂ interaction during polarization cycling and is expected to degrade the cycling endurance of the films further. Essentially, the nondegradation of P_r and E_C values up to 10⁹ cycles in tetragonal PLZT/YBCO/CeO₂/Si films infers that using a YBCO layer as the bottom electrode is as effective as using an RuO₂ electrode to suppress the generation of defects.^{3,4} Therefore, the fatigue of rhombohedral PLZT films using the same electrode materials implies that other factors contributed to degradation that is induced by polarization switching. The probable cause is periodic stress that is induced by polarization switching that is related to the piezoelectric nature of the films.

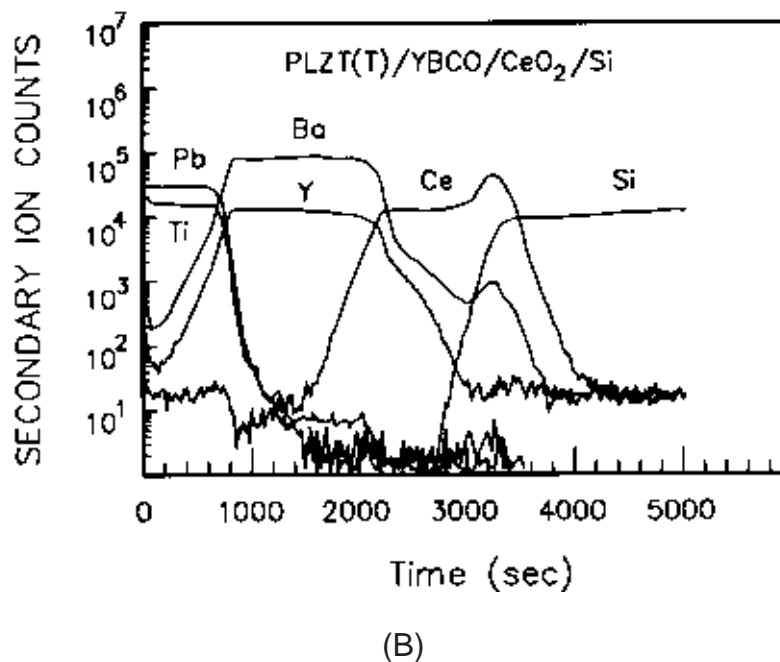
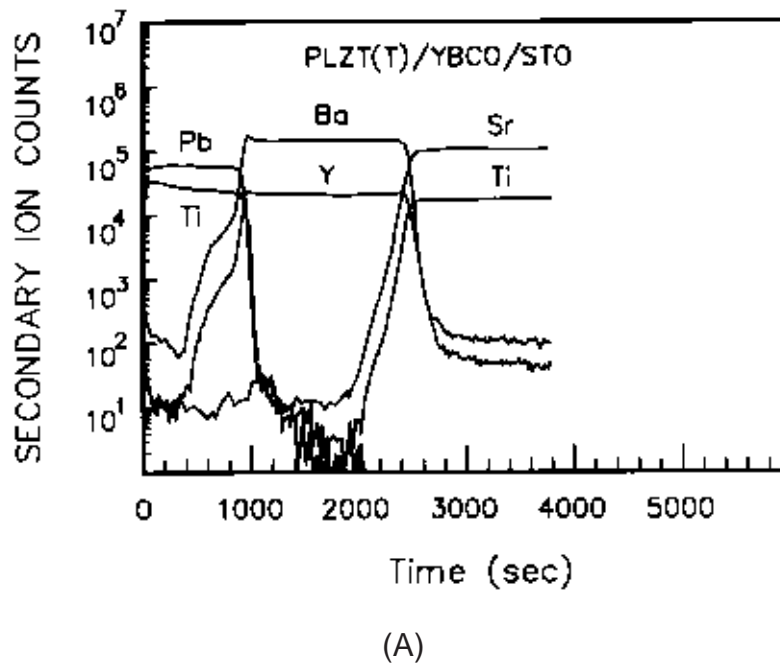


Fig. 4. SIMS spectra of rhombohedral PLZT films that have been deposited on (A) YBCO/STO and (B) YBCO/CeO₂/Si substrates at 500°C ($p_{O_2} = 10$ Pa).

IV. Summary

In summary, [00 \bar{l}] preferentially oriented PLZT thin films with either tetragonal or rhombohedral structures were obtained on YBCO-coated STO or YBCO/CeO₂-coated silicon substrates in the present study. The ferroelectric properties of those films then were examined. The PLZT films that were deposited onto YBCO/CeO₂/Si substrates possessed ferroelectric properties that were slightly inferior to those grown on YBCO/STO substrates, apparently because of appreciable PLZT–YBCO interaction and

the inferior crystallinity of the PLZT/YBCO/CeO₂/Si films. The tetragonal PLZT films not only possessed better ferroelectric properties than the rhombohedral films but also had superior fatigue properties, with respect to the polarization switching cycles. The properties of remnant polarization P_r and coercive field E_c of the tetragonal films ($(P_r)_T = 11.8 \mu\text{C}/\text{cm}^2$ and $(E_c)_T = 40 \text{ kV}/\text{cm}$) exhibited no significant degradation up to 10^9 polarization switching cycles; those of rhombohedral films (i.e., $(P_r)_R = 11.2 \mu\text{C}/\text{cm}^2$ and $(E_c)_R = 44.2 \text{ kV}/\text{cm}$) had already degraded to 80% of their initial values after 10^8 cycles.

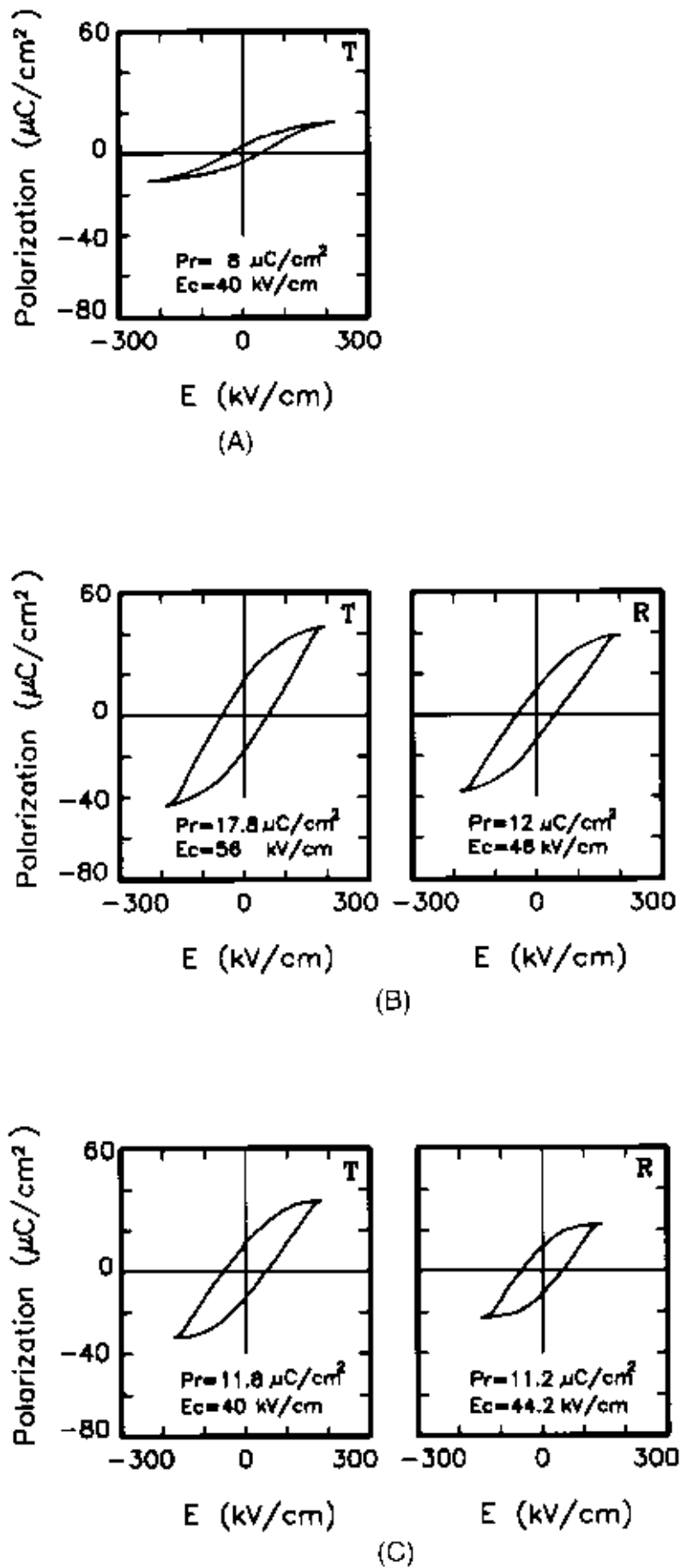


Fig. 5. Ferroelectric hysteresis loop of (A) PLZT/Pt(Ti)/Si, (B) YBCO/STO, and (C) YBCO/CeO₂/Si thin films that have been deposited at 500°C ($p_{O_2} = 10$ Pa).

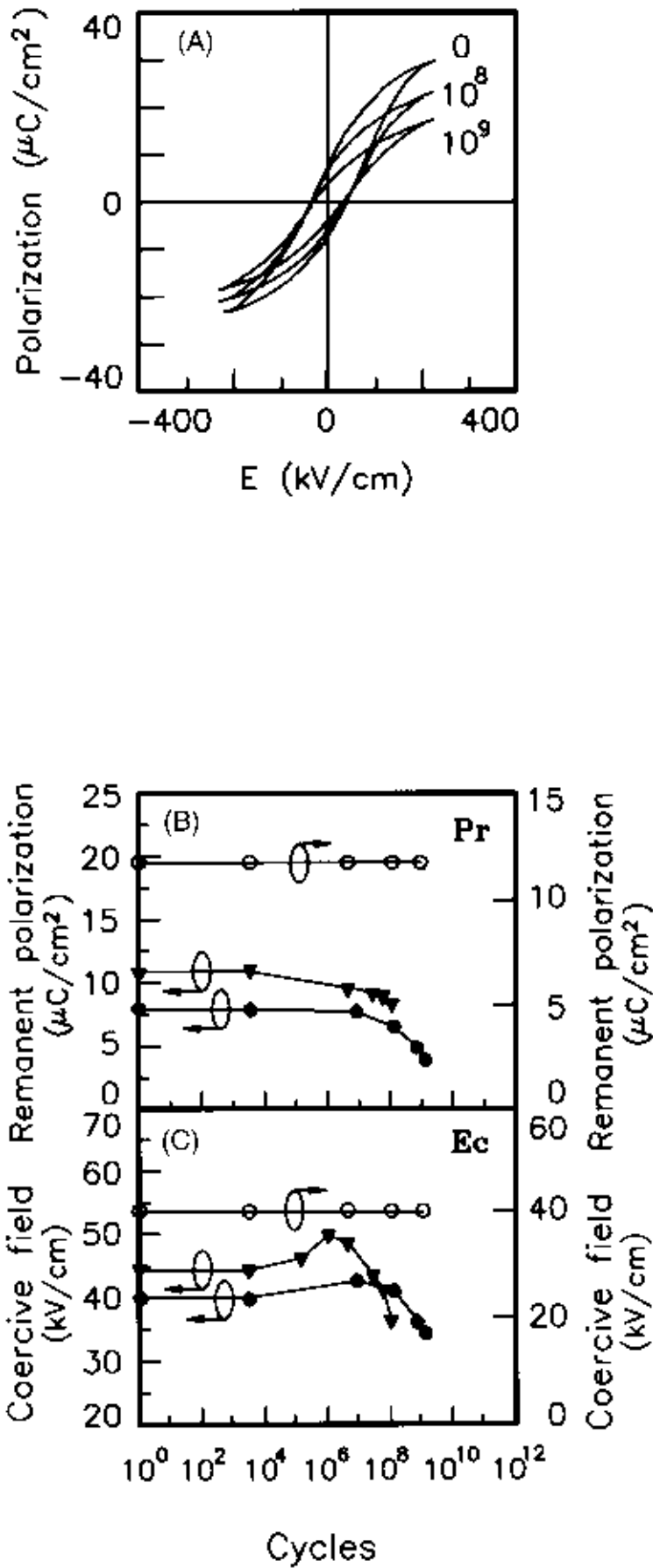


Fig. 6. (A) P - E hysteresis curve of PLZT/Pt(Ti)/Si films after 0, 10^8 , and 10^9 polarization switching cycles; the variation of (B) remnant polarization P_r and (C) coercive field E_c with the polarization switching cycles (\circ) T, tetragonal PLZT/YBCO/CeO₂/Si; (\blacktriangledown) R, rhombohedral PLZT/YBCO/CeO₂/Si; and (\bullet) P, PLZT/Pt(Ti)/Si.

Table II. Ferroelectric Properties of Rhombohedral (R) and Tetragonal (T) PLZT Films Deposited on Pt(Ti)/Si, YBCO/STO, or YBCO/CeO₂/Si Substrates

Substrate	Phase	Remnant polarization, P_r ($\mu\text{C}/\text{cm}^2$)	Coercive field, E_c (kV/cm)
Pt(Ti)/Si	T	8.0	40.0
YBCO/STO	R	12.0	46.0
YBCO/STO	T	17.8	56.0
YBCO/CeO ₂ /Si	R	11.2	44.2
YBCO/CeO ₂ /Si	T	11.8	40.0

References

- ¹B. K. Moon and H. Ishiwara, "Role of Buffer Layers in Epitaxial Growth of SrTiO Films on Silicon Substrates," *Jpn. J. Appl. Phys., Part 1*, **33** [3A] 1472–77 (1994).
- ²T. Mihara, H. Watanabe, and C. A. Paz de Araujo, "Characteristic Change Due to Polarization Fatigue of Sol-Gel Ferroelectric Pb(Zr_{0.4}Ti_{0.6})O₃ Thin-Film Capacitors," *Jpn. J. Appl. Phys., Part 1*, **33** [9B] 5281–86 (1994).
- ³H. N. Al-Shareef, K. R. Bellur, A. I. Kingon, and O. Auciello, "Influence of Platinum Interlayers on the Electrical Properties of RuO₂/Pb(Zr_{0.53}Ti_{0.47})O₃/RuO₂ Capacitor Heterostructures," *Appl. Phys. Lett.*, **66** [2] 239–41 (1995).
- ⁴H. N. Al-Shareef, A. I. Kingon, X. Chen, K. R. Bellur, and O. Auciello, "Contribution of Electrode and Microstructures to the Electrical-Properties of Pb(Zr_{0.53}Ti_{0.47})O₃ Thin-Film Capacitors," *J. Mater. Res.*, **9** [11] 2968 (1994).
- ⁵R. Dat, D. J. Lichtenwalner, O. Auciello, and A. I. Kingon, "Polycrystalline La_{0.5}Sr_{0.5}CoO₃/PbZr_{0.53}Ti_{0.47}O₃/La_{0.5}Sr_{0.5}CoO₃ Ferroelectric Capacitors on Platinized Silicon with No Polarization Fatigue," *Appl. Phys. Lett.*, **64** [20] 2673–75 (1994).

⁶J. Chen, M. P. Harmer, and D. M. Smyth, "Compositional Control of Ferroelectric Fatigue in Perovskite Ferroelectric Ceramics and Thin Films," *J. Appl. Phys.*, **76** [9] 5394–98 (1994).

⁷R. Ramesh, T. Sands, and V. G. Keramidas, "Template Approaches to Growth of Oriented Oxide Heterostructures on SiO₂/Si," *J. Electron. Mater.*, **23** [1] 19–23 (1994).

⁸R. Ramesh, T. Sands, V. G. Keramidas, and D. K. Fork, "Epitaxial Ferroelectric Thin Films for Memory Applications," *Mater. Sci. Eng., B*, **22**, 283–89 (1994).

⁹W. Pan, C. F. Yue, and S. Sun, "Domain Orientation Change Induced by Ferroelectric Fatigue Process in Lead Zirconate Titanate Ceramics," *Ferroelectrics*, **133**, 97–102 (1992).

¹⁰J. Lee, S. Esayan, A. Safari, and R. Ramesh, "Effect of Ultraviolet Light on Fatigue of Lead Zirconate Titanate Thin-Film Capacitors," *Appl. Phys. Lett.*, **65** [2] 254–56 (1994).

¹¹S. Thakoor, "Enhanced Fatigue and Retention in Ferroelectric Thin-Film Memory Capacitors by Post-Top-Electrode Anneal Treatment," *J. Appl. Phys.*, **75** [10] 5409–14 (1994).

¹²H. M. Duiker, P. D. Beale, J. F. Scott, C. A. Paz de Araujo, B. M. Melnick, J. D. Cuchiaro, and L. C. McMillan, "Fatigue and Switching in Ferroelectric Memories: Theory and Experiment," *J. Appl. Phys.*, **68** [11] 5783–91 (1990).

¹³S. Takahashi, "Multilayer Piezo-Ceramic Actuators and Their Applications"; pp. 349–51 in *Ferroelectric Ceramics: Tutorial Reviews, Theory, Processing, and Applications*. Edited by N. Setter and E. L. Colla. Birkhauser Verlag, Basel, Switzerland, 1993.

¹⁴M. H. Yeh, K. S. Liu, and I.-N. Lin, "Formation of the Secondary Phases in the Pb-Containing Perovskite Films by Pulsed Laser Deposition," *J. Mater. Res.*, **9** [9] 2379–85 (1994).

¹⁵M. C. Jiang and T. B. Wu, "The Effect of Electrode Composition on RF Magnetron Sputtering Deposition of Pb[(Mg_{1/3}Nb_{2/3})_{0.7}Ti_{0.3}]O₃ Films," *J. Mater. Res.*, **9** [7] 1879–86 (1994).

¹⁶B. Jaffe, W. R. Cook, and H. Jaffe, *Piezoelectric Ceramics*; pp. 16–20 and 135–48. Academic Press, London, U.K., 1971. □